VIROLOGICA SINICA 2015, 30 (6): 410–416
DOI: 10.1007/s12250-015-3651-y

RESEARCH ARTICLE

Application of an M13 bacteriophage displaying tyrosine on the surface for detection of Fe^{3+} and Fe^{2+} ions

Xiaohua Guo#, Chuncheng Niu#, Yunhua Wu, Xiaosheng Liang✉

College of Life Science &Hubei Provincial Key Laboratory for Protection and Application of Special Plants on Wuling Area, South-Central University for Nationalities, Wuhan 430074, China

Ferric and ferrous ion plays critical roles in bioprocesses, their influences in many fields have not been fully explored due to the lack of methods for quantification of ferric and ferrous ions in biological system or complex matrix. In this study, an M13 bacteriophage (phage) was engineered for use as a sensor for ferric and ferrous ions via the display of a tyrosine residue on the P8 coat protein. The interaction between the specific phenol group of tyrosine and Fe^{3+} / Fe^{2+} was used as the sensor. Transmission electron microscopy showed aggregation of the tyrosine-displaying phages after incubation with Fe^{3+} and Fe^{2+}. The aggregated phages infected the host bacterium inefficiently. This phenomenon could be utilized for detection of ferric and ferrous ions. For ferric ions, a calibration curve ranging from 200 nmol/L to 8 μmol/L with a detection limit of 58 nmol/L was acquired. For ferrous ions, a calibration curve ranging from 800 nmol/L to 8 μmol/L with a detection limit of 641.7 nmol/L was acquired. The assay was specific for Fe^{3+} and Fe^{2+} when tested against Ni^{2+}, Pb^{2+}, Zn^{2+}, Mn^{2+}, Co^{2+}, Ca^{2+}, Cu^{2+}, Cr^{3+}, Ba^{2+}, and K^{+}. The tyrosine displaying phage to Fe^{3+} and Fe^{2+} interaction would have plenty of room in application to biomaterials and bionanotechnology.

KEYWORDS M13 bacteriophage; tyrosine; display; ferric ion; ferrous ion; aggregation

INTRODUCTION

Currently, virus and virus-like particles (VLPs) are extensively used as biological templates because they can be easily functionalized by genetic engineering and chemical conjugation of their exterior surface coat proteins (Liu et al., 2012). Bacteriophage M13 is a filamentous virus (880 nm long and 6.6 nm wide for the wild-type virus) with a single-stranded DNA genome encapsulated by approximately 2700 copies of the major coat protein P8 and encased with five copies of four different minor coat proteins (P9, P7, P6, and P3) on the ends (Glucksman et al., 1992). This phage has been applied as a biological scaffold in biomaterials (Wu et al., 2011; Hess et al., 2013; Oh et al., 2014), imaging (Ghosh et al., 2012; Yi et al., 2012), biocatalysis (Neltner et al., 2010; Maeda et al., 2014), and drug delivery (Ghosh et al., 2012; De Porter and Mc Naughton, 2014).

Phage display is a method for the study of protein- or peptide-biological molecule interactions that utilize bacteriophages to connect peptides with the genetic information that encodes them (Smith, 1985; Guo et al., 2006). This connection between genotypes and phenotypes enables large libraries of peptides to be screened and amplified in a process called *in vitro* selection (Smith and Petrenko, 1997; Kehoe and Kay, 2005). Phage display libraries have been widely exploited for materials applications (Lee et al., 2002; Lee et al., 2006; Yoo et al., 2006; Zhang et al., 2015). Genetic modifications of phage M13 for phage display have focused on the major coat protein P8 and minor coat protein P3. Moreover, enzyme-catalyzed reactions coupled with phage display have recently been performed, facilitating the display of an unnatural group (3, 4-dihydroxyl-l-phenylalanine) on

Received: 16 September 2015, Accepted: 3 December 2015
Published online: 14 December 2015
# These authors contributed equally to this work.
✉ Correspondence:
Phone: +86-27-67842689, Fax: +86-27-67842689,
Email: liangxs@mail.scuec.edu.cn
ORCID: 0000-0003-1482-6914

phage M13, resulting in a universal binding affinity to inorganic materials by adhering to the major coat protein (Park et al., 2014).

Iron, particularly Fe^{3+}, is an essential transition metal for organisms and plays an important role in cellular metabolism and enzyme catalysis. Iron deficiency in the human body may lead to anemia, liver and kidney damage, diabetes, and heart diseases (Allen, 2002). Similarly, excessive Fe^{3+} in the body can also cause oxidative damage to tissues and fibrosis in various organs (Omara and Blakley, 1993). For microbes, the lack of Fe^{3+} ion results in slow or retarded growth. Additionally, excess Fe^{3+} may inhibit secondary metabolite production in microbe fermentation. Currently, a number of analytical techniques are available to detect Fe^{3+}. Among these, electrochemical methods, atomic absorption, ion chromatography, inductively coupled plasma-optical emission spectroscopy, fluorescence, and UV-Vis absorption spectroscopy are the most commonly used techniques. However, these methods require dedicated instruments. It is essential to develop simple and efficient methods without sophisticated instrumentation to detect Fe^{3+} in industrial, biological, and food samples.

Herein, we report a tyrosine-displaying M13 phage that aggregates under a wide range of concentration of ferric and ferrous ions, resulting in corresponding decreases in titers (Figure 1). This engineered phage could be used as a probe for ferric or ferrous ions without complicated instruments or reagents.

MATERIALS AND METHODS

Construction of a tyrosine-displaying phage

The M13KE phage vector was modified by preparing a cloning site for the display of P8, as described previously (Liu et al., 2012). A *Pst* I restriction site was cre-

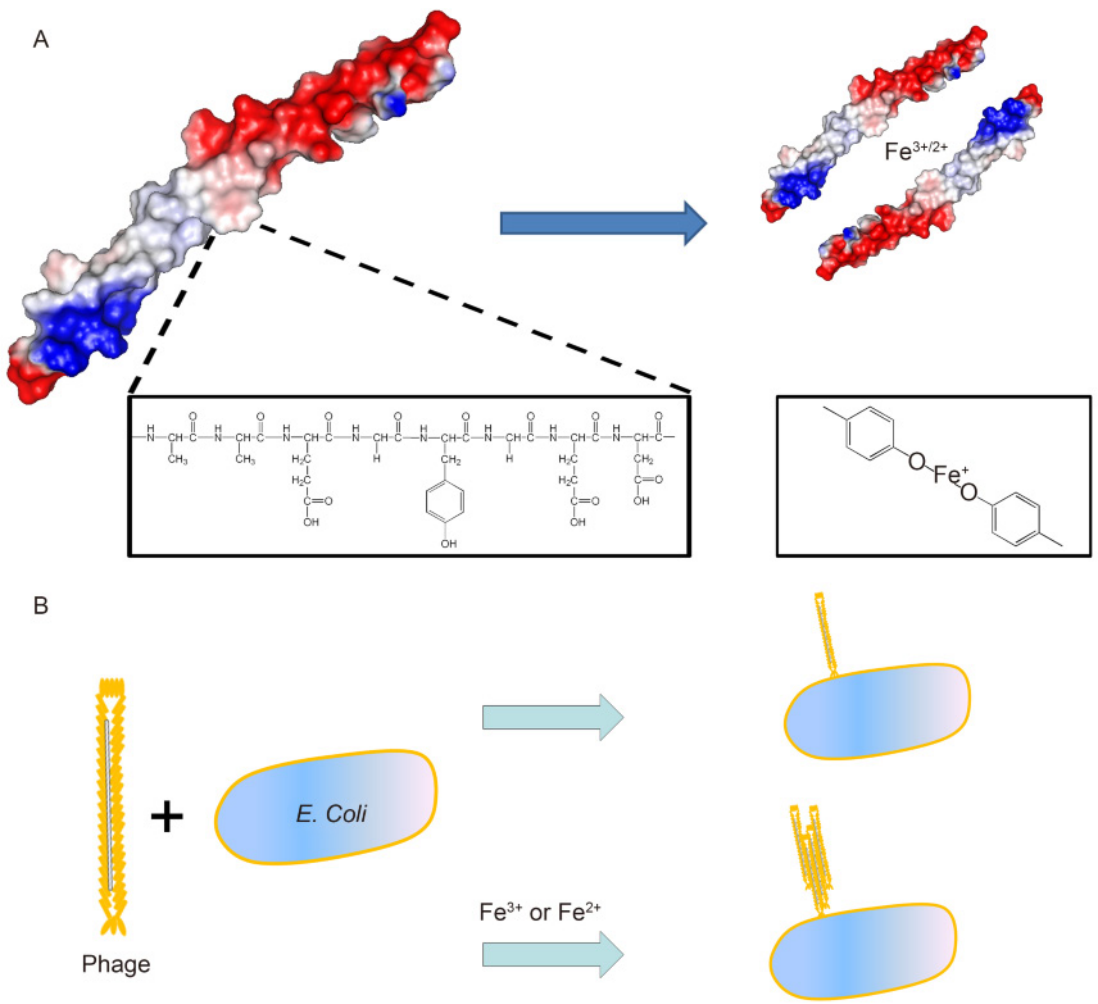

Figure 1. Schematic illustrations of (A) P8 coat protein displaying tyrosine and the tyrosine-Fe^{3+}/Fe^{2+} interaction and (B) titer-decreasing phenotypic characteristics associated with the Fe^{3+} and Fe^{2+} tyrosine interaction.

ated by mutating T to A at position 1372, a *Bam*H I site was created by mutating C to G at position 1381, and a *Pst* I site at position 6246 was deleted by mutation. Site-directed mutagenesis was performed using overlap extension polymerase chain reaction (PCR). The sequence encoding the tyrosine-containing peptide was cloned into the modified phage vector using *Pst* I and *Bam*H I. Two primers were designed to insert YG into the P8 coat protein: 5′-CGCTGCAGAGGGTTACGGTGAG-GATCCCGCA-3′ and 5′-GATCCTCACCGTAAC-CCTCTGCA-3′. To engineer the tyrosine-displaying phage, the mutated M13KE phage vector (New England Biolabs, Ipswich, USA) was digested with *Pst* I and *Bam*H I. The purified long fragment was recircularized with the above primers via overnight ligation at 16 °C using T4 DNA ligase (TaKaRa Bio, Shiga, Japan). The ligated DNA vector was transformed into competent *E. coli* K12 ER2738 (New England Biolabs, Ipswich, USA) cells that were plated on LB agar plates containing 10 μg/mL tetracycline after mixing with top agar. The amplified phage vector was verified by DNA sequencing. The resulting phage vector was named M13KE-tyr and could be used for detection of ferric and ferrous ions.

Transmission electron microscopy (TEM)

The *E. coli* strain was infected with phage for at least 12 h at 37 °C. The cultures were centrifuged at 12,000 × g for 20 min, and the phage was precipitated from the supernatant at 4 °C with the addition of one-fifth of the supernatant volume of 20% PEG 8000 / 2.5 mol/L NaCl solution. After centrifugation at 13,500 × g for 20 min, the pellet was re-suspended with 1 mL sterile water. One hundred microliters of the phage suspension was incubated with ferric ion or ferrous ion for 2 h at room temperature at different final ion concentrations. The untreated phage suspension was used as a control. A 10-μL 10^{12} pfu/mL phage suspension was incubated with 8 μmol/L ferric or ferrous ion for 2 h at room temperature. Next, 50 μL of *E. coli* K12 ER2738 at an optical density (OD) of 1 was added and incubated for 10 min. Drops of the mixture were prepared for TEM imaging.

Carbon film-coated grids were floated for 10 min on drops of the sample placed on a parafilm surface. Excess solution was removed from the grid by carefully wiping the edge of the grid with a filter paper. For negative staining, the grids were then floated on drops of 2% phosphotungstic acid for 15 min. Excess fluid was removed in the same manner as described above, and the grids were allowed to dry overnight. The images were captured using TEM (H7000; Hitachi, Tokyo, Japan).

Drawing the standard curve

Purified KE-Tyr and M13KE strains were serially diluted to an appropriate concentration of 10^5 pfu/mL and incubated with ferric ion for 2 h at a final concentration of 8 μmol/L. Moreover, the diluted KE-Tyr strain (concentration of 10^5 pfu/mL) was incubated with different concentrations of ferric ion or ferrous ion for 2 h. Untreated strains were used as a control. The plaques were counted after forming on double-agar plates during culture at 37 °C, and the percent inhibition was calculated.

Influence of various foreign ions

Phage preparations were diluted to a concentration of 10^5 pfu/mL and incubated with various metal ions for 2 h at room temperature at a final concentration of 5 μmol/L. Untreated strains were used as a control. The percent inhibition was calculated, and a histogram was plotted.

RESULTS

A phage with a YG peptide on the N terminus of the P8 coat protein (termed KE-Tyr phage) was engineered to introduce a tyrosine residue. The insert region on the P8 coat protein had the sequence AAEGYGE. The KE-Tyr phages were incubated with different concentrations of ferric or ferrous ions for 2 h, and their morphologies were observed using TEM. As shown in the TEM images, following incubation with ferric and ferrous ions, the KE-Tyr phage aggregated side by side into bunch-like structures (Figure 2A–2F). In contrast, the KE-Tyr phages were randomly distributed without ferric ions, as shown in Figure 2G. TEM characterization of the attachment of the packed M13 phage to host bacteria demonstrated that the host bacteria were adhered via tyrosine-displaying phages previously incubated with 8 μmol/L ferric or ferrous ions. As shown in Figure 3, the aggregation of the phage resulted in many phages coming in contact with one host bacterial cell.

To evaluate the changes in titers, the wild-type phages M13KE and the tyrosine-displaying phages KE-Tyr were titrated after incubation with different concentrations of ferric or ferrous ions. KE-Tyr phages were titrated with or without 8 μmol/L ferric ion to verify that ferric ion could decrease the titer of the phage through a method other than phage aggregation on the nanoscale. In contrast, M13KE phages, which possessed no tyrosine residues on the outer surface of the major coat protein, were titrated with or without 8 μmol/L ferric ions. Under this condition, titration of KE-Tyr yielded 20.4% remaining, whereas titration of KE yielded 92.9% remaining (Figure 4A).

A freshly prepared ferric chloride solution was sequentially diluted to generate samples for titration of the phage. In these assays, KE-Tyr phages were titrated with ferric or ferrous ions under different concentrations. To ensure that the results were stable and reliable, over 10 parallel experiments were performed for each concentration of ferric ion (Figure 4C, 4D).

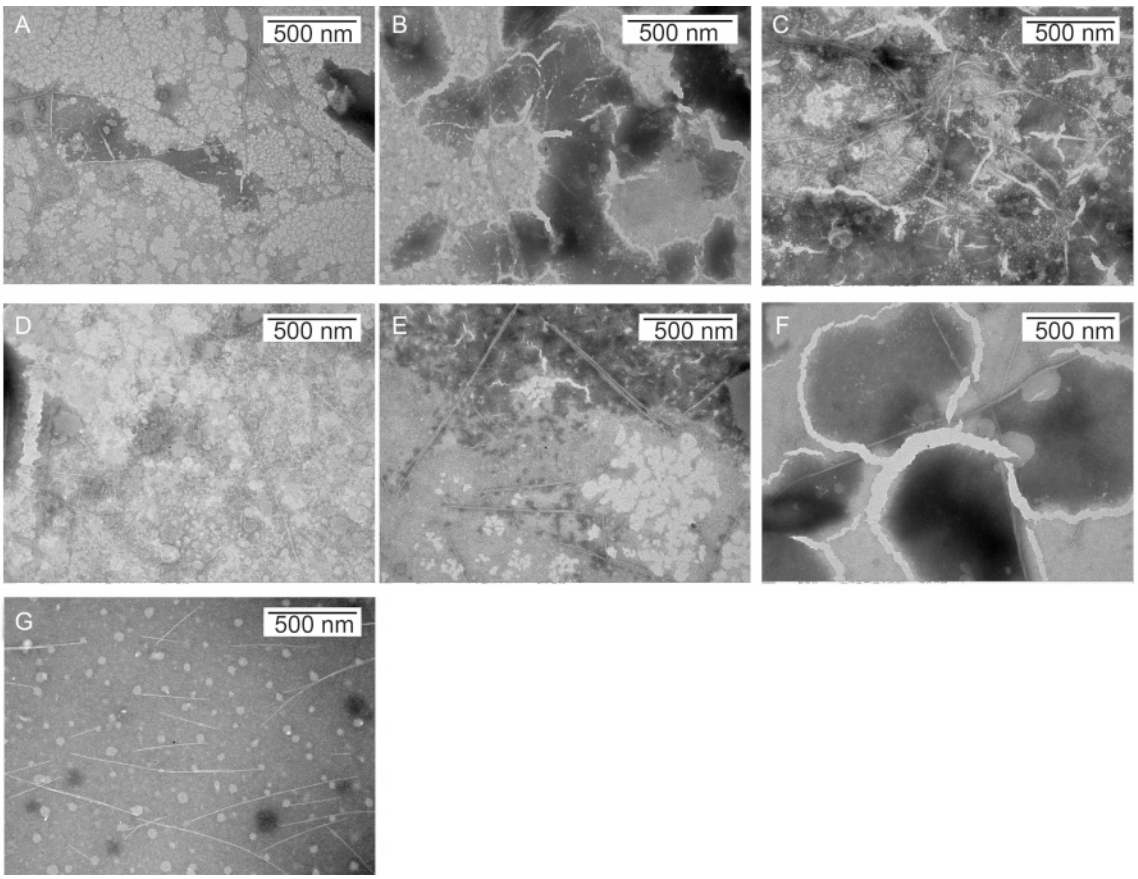

Figure 2. TEM image of the KE-Tyr phage incubated with 0.2, 2, or 8 μmol/L Fe^{3+} (A–C) or 0.2, 2, or 8 μmol/L Fe^{2+} (D–F) for 2 h. The control was the TEM image of KE-Tyr phage without Fe^{3+}or Fe^{2+} (G). Samples were stained with 2% phosphatotungstic acid.

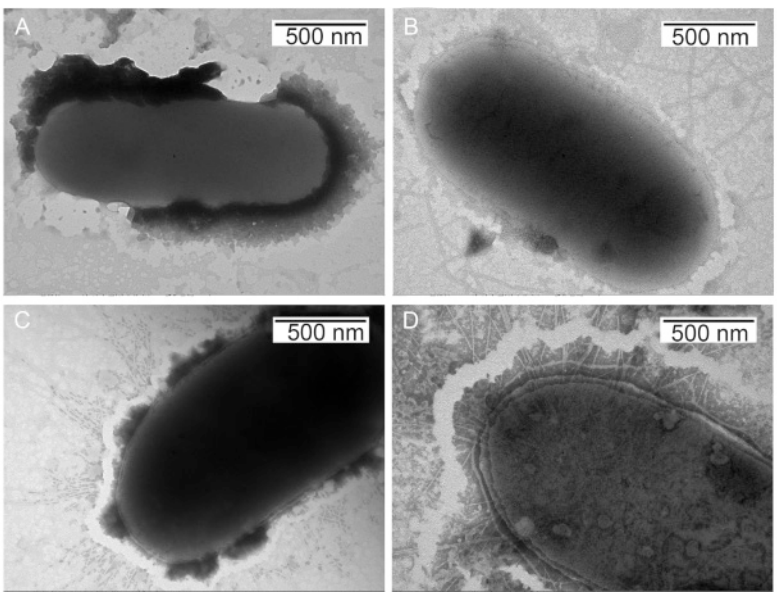

Figure 3. TEM images of the of host bacteria (A), host bacterium attached to the KE-Tyr phages (B), host bacterium with ferric ion at 8 μmol/L attached to the KE-Tyr phages (C), and host bacterium with ferrous ion at 8 μmol/L attached to the KE-Tyr phages (D). Samples were negatively stained with 2% phosphatotungstic acid.

The remaining percent of phage titers after incubation with Fe^{3+}/Fe^{2+} ions was exponentially related to the ion concentration. As shown in Figure 4D, the remaining percentages of the phage were linearly plotted with the natural logarithm of the ferric ion concentration. The phage responses to ferric ions were calibrated from 200 nmol/L to 8 μmol/L with a correlation coefficient of 0.9945. A detection limit of 58 nmol/L was acquired (S/N = 3). The sanitary security limit for the Fe^{3+} ion was restricted to 2 mg/L (35 μmol/L) by the World Health Organization (WHO). The detection limit achieved in this study was much lower than the sanitary security limit of the WHO. For ferrous detection, a detection limit of 641.7 nmol/L was acquired (S/N = 3) with a calibrated range from 800 nmol/L to 8 μmol/L (Figure 4C).

To test the specificity of the phage sensor to several common metal ions, including Ni^{2+}, Pb^{2+}, Zn^{2+}, Mn^{2+}, Co^{2+}, Ca^{2+}, Cu^{2+}, Cr^{3+}, Ba^{2+}, and K^{+}, were selected as interferents to study the specificity of this phage sensor. The concentration of all tested ions was 5 μmol/L. As shown in Figure 4B, marked decreases were observed in the presence of Fe^{3+} and Fe^{2+}, while other responses of the biosensor to interferents were similar to the blank control, except for Pb^{2+} and Zn^{2+}. The titers of the phage dropped to 43% and 26% after 2 h of incubation with 5 μmol/L Pb^{2+} and Zn^{2+}, respectively.

DISCUSSION

In this study, we engineered the tyrosine-displaying M13 bacteriophage to have the AAEGYGE moiety, which was rich in glycine and alanine. The introduction of alanine and glycine was helpful to reduce steric hindrance. The YG peptide inserted into the glutamate

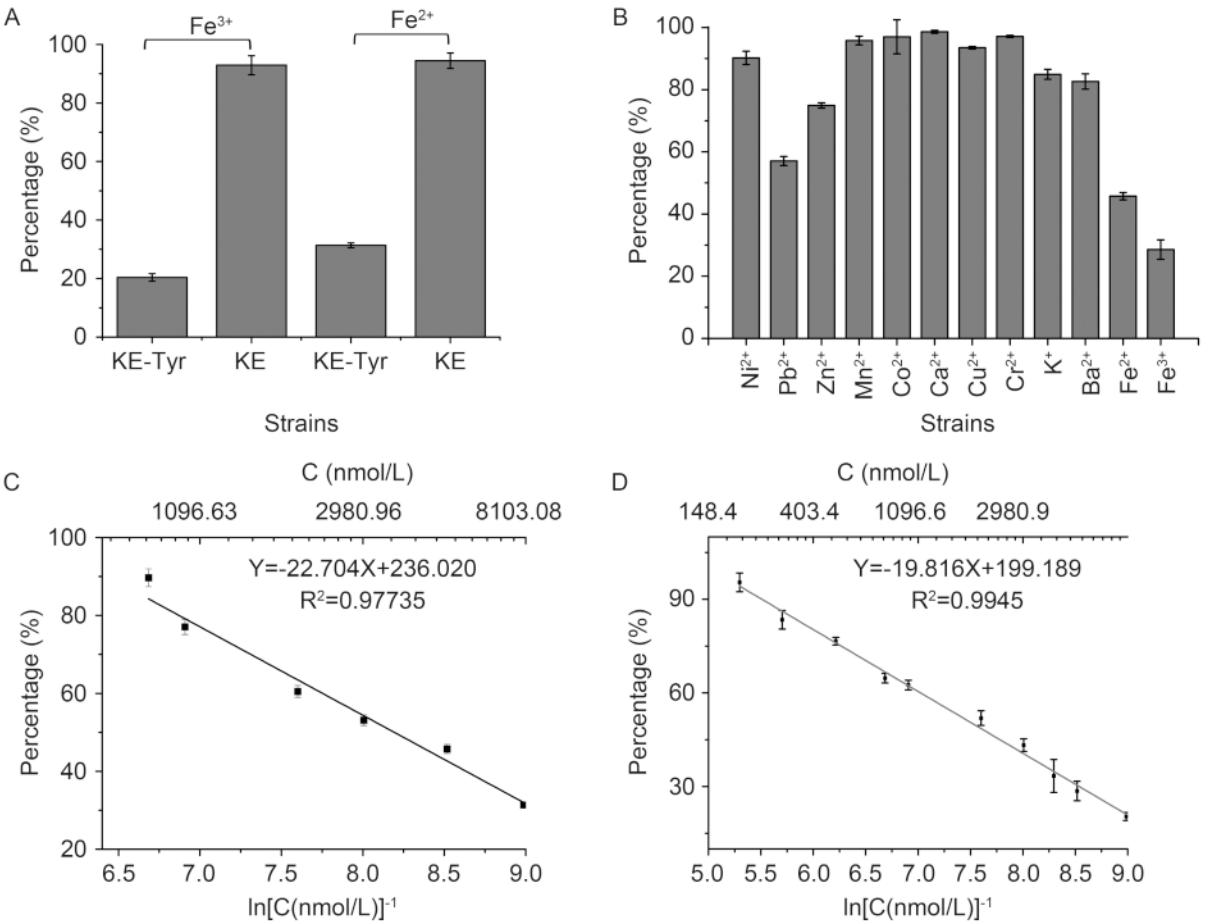

Figure 4. (A) Relative titer histograms for KE-Tyr and KE phages after incubation with ferric and ferrous ions at 8 μmol/L for 2 h. (B) Relative titer contrast bars were used to investigate the interference effect of other metal ions (Ni^{2+}, Pb^{2+}, Zn^{2+}, Mn^{2+}, Co^{2+}, Ca^{2+}, Cu^{2+}, Cr^{3+}, Ba^{2+}, and K^{+}) on the detection of Fe^{3+}. The phage incubation concentration was 10^5 pfu/mL. The ion concentration was 5 μmol/L. (C) The calibrated curve of KE-Tyr phage relative titers versus the logarithm of the ferrous ion concentration (phage incubation concentration 10^5 pfu/mL). (D) The calibrated curve of KE-Tyr phage relative titers versus the logarithm of ferric ion concentrations (phage incubation concentration 10^5 pfu/mL).

rich region was used to attract metal ions and the tyrosine- displaying phages aggregated side by side after incubation with Fe^{3+} and Fe^{2+}. Such aggregation of most of the phages blocked amplification of the phages through infection. Similar analyses showed that the titers of the phages were influenced by ferric and ferrous ions. Thus, the phage constructed herein could be used to detect ferric and ferrous ions and may have applications in a range of fields.

Several common metal ions, including Ni^{2+}, Pb^{2+}, Zn^{2+}, Mn^{2+}, Co^{2+}, Ca^{2+}, Cu^{2+}, Cr^{3+}, Ba^{2+}, and K^{+}, were tested as interferents to assess the specificity of the phage sensor. Although the relative titers were more than twice those of the phages incubated with Fe^{3+}, both Pb^{2+} and Cd^{2+} are heavy ions that may denature proteins. However, no obvious decrease in titers was observed when the phage was incubated with 5 μmol/L Cd^{2+}. This implied that the denaturation of proteins was not the key factor responsible for the decreased phage titers. Instead, the decreased titers of phages incubated with Pb^{2+} and Zn^{2+} may be explained by electrostatic interactions or chelation. Selectivity was analyzed at a concentration of 5 μmol/L, which is near the upper range of phage sensor detection. In the intermediate concentration of the detection range, the interference of other ions was negligible. These results suggested that this method had excellent selectivity for Fe^{3+} and Fe^{2+}, which could be attributed to the high selectivity of Fe^{3+} phenol group interactions.

Because of the requirement for bacteria culture, the method presented herein was time consuming. However, no specialized instruments were required as the method was based on plaque counting. During antibiotic fermentation, the ferric ion could influent the titer of antibiotics. For example, penicillin fermentation is inhibited in the presence of more than 20 μg/mL ferric ion. For gentamycin, fermentation is affected in the presence of more than 15 μg/mL ferric ion. Thus, this method provides a simple sensor for ferric and ferrous ions in biochemical laboratories and for industrial fermentation processes.

In summary, in this study, we designed a phage sensor based on genetic modification of viral coating protein for ferric and ferrous ions detection. A tyrosine residue was displayed on the P8 of phage M13. TEM results showed that tyrosine-displaying phages aggregated after incubation with ferric or ferrous ions. Titration assays indicated that the aggregated phage was much less infective. The specific interaction between the ferric ion and the phenol group of the tyrosine ensured the high selectivity of the sensor. Additionally, this phage ions interaction could be further applied for biocompatible materials and signal conversion of phage based ELISA.

ACKNOWLEDGMENTS

This work was funded by the National Natural Science Foundation of China (No. 31300829), Natural Science Foundation of Hubei Province of China (No. 2014CFC1117), and Open Research Fund Program of the State Key Laboratory of Virology of China (No. 2015IOV002).

COMPLIANCE WITH ETHICS GUIDELINES

The authors declare that they have no conflict of interest. This article does not contain any studies with human or animal subjects performed by any of the authors.

AUTHOR CONTRIBUTIONS

XL designed the experiments and cloned the tyrosine displaying phage. XG purified and titrated the phage. CN performed the ferric and ferrous ions detection and phage characterization. YW analyzed the data. All authors read and approved the final manuscript.

REFERENCES

Allen LH, 2002. Iron supplements: scientific issues concerning efficacy and implications for research and programs. J Nutr, 132: 813S–819S.

DePorter SM, McNaughton BR. 2014. Engineered M13 bacteriophage nanocarriers for intracellular delivery of exogenous proteins to human prostate cancer cells. Bioconjug Chem, 25: 1620–1625.

Ghosh D, Kohli AG, Moser F, Endy D, Belcher AM. 2012. Refactored M13 bacteriophage as a platform for tumor cell imaging and drug delivery. ACS Synth Biol, 1: 576–582.

Glucksman MJ, Bhattacharjee S, Makowski L. 1992. Three-dimensional structure of a cloning vector. X-ray diffraction studies of filamentous bacteriophage M13 at 7 A resolution. J Mol Biol, 226: 455–470.

Guo YC, Zhou YF, Zhang XE, Zhang ZP, Qiao YM, Bi LJ, Wen JK, Liang MF, Zhang JB. 2006. Phage display mediated immuno-PCR. Nucleic Acids Res, 34: e62.

Hess GT, Guimaraes CP, Spooner E, Ploegh HL, Belcher AM. 2013. Orthogonal labeling of M13 minor capsid proteins with DNA to self-assemble end-to-end multiphage structures. ACS Synth Biol, 2: 490–496.

Kehoe JW, Kay BK. 2005. Filamentous phage display in the new millennium. Chem Rev, 105: 4056–4072.

Lee SK, Yun DS, Belcher AM. 2006. Cobalt ion mediated self-assembly of genetically engineered bacteriophage for biomimetic Co-Pt hybrid material. Biomacromolecules, 7: 14–17.

Lee SW, Mao C, Flynn CE, Belcher AM. 2002. Ordering of quantum dots using genetically engineered viruses. Science, 296: 892–895.

Liu Z, Qiao J, Niu Z, Wang Q. 2012. Natural supramolecular building blocks: from virus coat proteins to viral nanoparticles. Chem Soc Rev, 41: 6178–6194.

Maeda Y, Javid N, Duncan K, Birchall L, Gibson KF, Cannon D, Kanetsuki Y, Knapp C, Tuttle T, Ulijn RV, Matsui H. 2014. Discovery of catalytic phages by biocatalyticself-assembly. J Am Chem Soc, 136: 15893–15896.

Neltner B, Peddie B, Xu A, Doenlen W, Durand K, Yun DS,

Speakman S, Peterson A, Belcher A. 2010. Production of hydrogen using nanocrystalline protein-templated catalysts on m13 phage. ACS Nano, 4: 3227–3235.

Oh D, Qi J, Han B, Zhang G, Carney TJ, Ohmura J, Zhang Y, Shao-Horn Y, Belcher AM. 2014. M13 virus-directed synthesis of nanostructured metal oxides for lithium-oxygen batteries. Nano Lett, 14: 4837–4845.

Omara FO, Blakley BR. 1993. Vitamin E is protective against iron toxicity and iron-induced hepatic vitamin E depletion in mice. J Nutr, 123: 1649–1655.

Park JP, Do M, Jin HE, Lee SW, Lee H. 2014. M13 bacteriophage displaying DOPA on surfaces: fabrication of various nanostructured inorganic materials without time-consuming screening processes. ACS Appl Mater Interfaces, 6: 18653–18660.

Smith GP. 1985. Filamentous fusion phage: novel expression vectors that display cloned antigens on the virion surface. Science, 228: 1315–1317.

Smith GP, Petrenko VA. 1997. Phage Display. Chem Rev, 97: 391–410.

Wu L, Lee LA, Niu Z, Ghoshroy S, Wang Q. 2011. Visualizing cell extracellular matrix (ECM) deposited by cells cultured on aligned bacteriophage M13 thin films. Langmuir, 27: 9490–9496.

Yi H, Ghosh D, Ham MH, Qi J, Barone PW, Strano MS, Belcher AM. 2012. M13 phage-functionalized single-walled carbon nanotubes as nanoprobes for second near-infrared window fluorescence imaging of targeted tumors. Nano Lett, 12:1176–1183.

Yoo PJ, Nam KT, Qi J, Lee SK, Park J, Belcher AM, Hammond PT. 2006. Spontaneous assembly of viruses on multilayered polymer surfaces. Nat Mater, 5: 234–240.

Zhang X, Hou Y, He W, Yang G, Cui J, Liu S, Song X, Huang Z. 2015. Fabricating high performance lithium-ion batteries using bionanotechnology. Nanoscale, 7: 3356–3372.